Acta Crystallographica Section D
Biological Crystallography
ISSN 0907-4449

Purification, crystallization and X-ray analysis of Hibiscus chlorotic ringspot virus

Kian-Chung Lee,[a] Daina Lim,[b] Sek-Man Wong[b] and Terje Dokland[a]*

[a]Institute of Molecular and Cell Biology, 30 Medical Drive, Singapore 117609, Singapore, and [b]Department of Biological Sciences, 14 Science Drive 4, National University of Singapore, Singapore 117543, Singapore

Correspondence e-mail: dokland@imcb.nus.edu.sg

Received 3 March 2003
Accepted 27 May 2003

Hibiscus chlorotic ringspot virus (HCRSV), a Carmovirus, occurs worldwide and induces chlorotic ringspots on leaves, stunting and flower distortion in *Hibiscus* species, including kenaf. The HCRSV capsid has $T = 3$ icosahedral symmetry and contains 180 copies of the coat protein. A virus yield of 48–70 mg per 100 g of infected kenaf leaves was achieved with an improved purification scheme involving sucrose-cushion and sucrose density-gradient centrifugation. The virus was crystallized using PEG 8000 and 2,3-butanediol as co-precipitants. The crystals belonged to the cubic space group $P23$, with unit-cell parameter $a = 392$ Å, and diffracted X-rays to at least 4.5 Å resolution.

1. Introduction

Hibiscus chlorotic ringspot virus (HCRSV; ICTV 74.0.2.0.008) is a monopartite single-stranded RNA virus first described in a hibiscus cultivar imported to the United States from El Salvador. The virus infects kenaf (*Hibiscus cannabinus* L.), a woody plant of interest to the woodpulp industry in the United States (Johnson, 2001), and is found worldwide where hibiscus is cultivated (Waterworth *et al.*, 1976), including Singapore (Wong & Chng, 1992). The HCRSV genome contains 3911 nucleotides with seven major open reading frames (Huang *et al.*, 2000). Based on virion morphology, genome organization, physico-chemical properties and amino-acid sequence, the virus is classified in the genus *Carmovirus* in the family *Tombusviridae*.

HCRSV has a 30 nm diameter icosahedral capsid with $T = 3$ symmetry (Caspar & Klug, 1962) containing 180 copies of a 38 kDa coat protein (CP). The capsid encapsidates either the full-length genomic RNA (3.9 kbp) or one of the two putative subgenomic RNAs (1.5 kbp and 1.7 kbp; Huang *et al.*, 2000).

The structures of two carmoviruses, turnip crinkle virus (TCV) and tomato bushy stunt virus (TBSV), have been determined to near-atomic resolution by X-ray crystallography (Olson *et al.*, 1983; Hogle *et al.*, 1986). The CPs consist of three domains, of which the shell-forming (S) domain and the protruding (P) domain both have the eight-stranded anti-parallel β-sandwich motif found in many virus structures. An internal RNA-binding (R) domain is disordered in the X-ray structures. The CP of HCRSV shares approximately 28% sequence identity with the CPs of TCV and TBSV.

In this paper, we describe the purification, crystallization and preliminary X-ray analysis of HCRSV from kenaf. The HCRSV crystals diffracted to least 4.5 Å resolution. Analysis of the diffraction data suggests that the space group is $P23$, with two particles in the unit cell rotated by 90° relative to each other. Further work is under way to obtain the atomic resolution structure of HCRSV.

2. Methods

2.1. Virus source

HCRSV was obtained from an infected *H. rosa-sinensis* exhibiting chlorotic leaf spots. The infected plant tested as being HCRSV-positive by enzyme-linked immunosorbent assay (ELISA). A single local lesion was serially transferred and propagated in kenaf cultivar EG-41. The infected kenaf plants were maintained in growth chambers at a temperature of 298 K, a relative humidity of 75% and with 18 h of light per day.

2.2. Purification

Frozen inoculated kenaf leaves were homogenized using a Waring Blender in three volumes (w/v) of extraction buffer (0.2 M NaOAc pH 5.4, 50 mM NaCl, 20 mM $CaCl_2$, 5 mM EDTA) containing 0.1% β-mercapto-ethanol. All subsequent procedures were carried out at 277 K unless otherwise stated. The slurry was centrifuged at 12 000g for 15 min. The supernatant was filtered through Miracloth (United States Biochemical, Cleveland, OH, USA) and kept on ice. The plant debris pellet was re-extracted with extraction buffer to maximize the virus yield. The supernatant was pooled and one volume of saturated ammonium sulfate solution was added before incubation for 1–2 h on ice. Centrifugation was performed at 12 000g for 20 min and the

resulting pellet was resuspended overnight at 277 K in resuspension buffer (0.05 *M* NaOAc pH 5.4, 50 m*M* NaCl, 20 m*M* $CaCl_2$, 5 m*M* EDTA) supplemented with 0.1% β-mercaptoethanol and 1% Triton-X100.

The suspension was centrifuged at 12 000*g* for 15 min. The supernatant was collected and layered onto a 10% sucrose cushion with resuspension buffer before ultracentrifugation at 100 000*g* for 3 h using an SW28 rotor (Beckman Coulter Inc., Fullerton, CA, USA). A small volume of resuspension buffer was added to resuspend the pellet overnight at 277 K. This was followed by centrifugation at 12 000*g* for 3 min to remove insoluble debris. The supernatant was collected and layered onto a 10–40% sucrose gradient in resuspension buffer before ultracentrifugation at 100 000*g* for 3 h in an SW28 rotor. The visible virus band was collected using a glass Pasteur pipette. After threefold to fourfold dilution with resuspension buffer, the purified virus was pelleted at 100 000*g* for 3 h using a swing-out rotor. The virus pellet was resuspended in a small amount of virus buffer (10 m*M* NaOAc pH 5.4, 50 m*M* NaCl, 5 m*M* $CaCl_2$) and stored at 277 K. The virus concentration was calculated using an extinction coefficient of $\varepsilon_{260\mathrm{nm}} = 5.0$ (Morris & Carrington, 1988).

2.3. Electron microscopy

Purified virus was placed on carbon film on 400-mesh copper grids, negatively stained with 1.0% PTA pH 7.2 and examined in a Jeol JEM-1030 TEM operated at 100 kV with magnification of 50 000×. In order to view virus particles in the crystals, a fine pipette tip was used to crush the virus crystals in the crystallization drops. A small amount of the crushed crystals was placed onto EM grids and negatively stained with 1.0% uranyl acetate before TEM examination.

2.4. Crystal growth

Crystallization conditions were screened by the hanging-drop vapour-diffusion method using Linbro multiwell crystallization plates (Hampton Research, Laguna Niguel, CA, USA). The drops were set up with 2 µl of purified virus and 2 µl of crystallization well buffer [0.1 *M* 2-(*N*-morpholino)ethanesulfonic acid (MES) pH 6.0]. Different concentrations of ammonium sulfate, PEG 6000 and PEG 8000 and different pH values were used to determine the precipitation conditions. A range of protein concentrations between 15 and 90 mg ml^{-1} were used. Crystallization trials were set up at 288 K. Conditions that gave crystalline precipitates in the hanging drops were identified and optimized further.

2.5. Data collection

Glycerol, 2-methyl-2,4-pentanediol (MPD) and 2,3-butanediol were used in cryoprotectant trials. Crystals were soaked in ascending concentrations of cryoprotectant (increments of 5% from 5 to 30%) in glass depression wells and then frozen directly in the 100 K N_2-gas stream from an Oxford Cryosystems cryostream. Synchrotron X-ray data were collected at station ID29 at the European Synchrotron Radiation Facility (ESRF), Grenoble using a 30 cm ADSC Quantum Q210 CCD detector. A crystal-to-detector distance of 400 mm, an oscillation angle of 0.3° at 1.033 Å wavelength and exposure times of 2–4 s were set as diffraction parameters (Table 1). Diffraction data were processed and scaled using the programs *DENZO* and *SCALEPACK* (Otwinowski & Minor, 1997). Self-rotation functions were calculated with the program *GLRF* (Tong & Rossmann, 1997).

3. Results and discussion

Systemic necrotic and chlorotic ringspots were observed in kenaf leaves approximately 10 d after inoculation. The growth of kenaf seedlings was significantly reduced in comparison to non-inoculated seedlings. Determination of peak virus titre by ELISA indicated that the virus titre in the infected kenaf leaves fluctuated in cycles and reached a peak at intervals of approximately every 15 d (results not shown). As such, infected leaves were harvested 15 d after inoculation and stored at 193 K prior to virus purification.

HCRSV was initially purified according to the method described by Hurtt (1987), which involves a combination of differential centrifugation and CsCl density-gradient centrifugation. However, the yields and purity obtained by this method were rather low. By using a combination of sucrose-cushion and sucrose density-gradient purification, we obtained yields of 48–70 mg of highly purified virus per 100 g of infected leaves, a significant improvement over the original protocol. After centrifugation through a 10% sucrose cushion, the virus pellet was pale greenish in appearance, indicating contamination with plant material. However, after sucrose-gradient centrifugation the viral particles formed a distinct band and a clear translucent pellet was obtained after concentration by centrifugation. The $A_{260/280\ \mathrm{nm}}$ of the purified virus was 1.76 (uncorrected for light scattering). Examination of purified HCRSV virions in the TEM revealed isometric particles that measured approximately 30 nm in diameter (Fig. 1).

Table 1
Statistics of data evaluation of the HCRSV crystal.

Data in parentheses are for the highest resolution bin.

X-ray source	ESRF ID29
Detector	ADSC Q210
Crystal-to-detector distance (mm)	400
Wavelength (Å)	1.033
Oscillation angle (°)	0.3
No. of frames	116
Total No. of reflections	418608
Unique reflections	112179
Resolution (Å)	42.0–4.5 (4.7–4.5)
Completeness (%)	94.4 (94.9)
Redundancy	3.7
R_{merge}	0.165 (0.742)
$\langle I/\sigma(I)\rangle$	6.1 (1.3)
Space group	*P*23
Unit-cell parameter (Å)	$a = 392.0$
Mosaicity	0.36

Crystallization trials containing various concentrations of PEG 6000 and PEG 8000 produced crystals that were bipyramidal in shape, but crystals grown in PEG 8000 exhibited sharper facets in comparison to those grown in PEG 6000. No crystals were obtained when ammonium sulfate was used as precipitant. A range of pH values was tested, but crystals only formed at pH 6. Small crystals were obtained within 2–3 h of setting up the crystallization trays and grew to dimensions of between 0.2 and 0.3 mm in 2 d. However, the crystals had a tendency to disintegrate and subsequently disappeared within a week. In order to prevent this melting phenomenon, cryoprotectants such as glycerol, MPD or 2–8% 2,3-butanediol were added directly into the crystallization buffer at concentrations between 2 and 8%. Addition of these compounds delayed the melting up to 3–4 weeks and allowed the

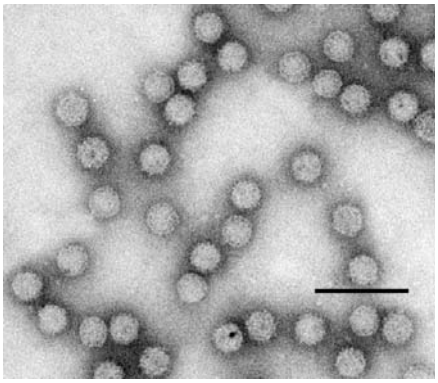

Figure 1
Purified HCRSV particles negatively stained with 1% PTA and viewed in the TEM. The bar represents 100 nm.

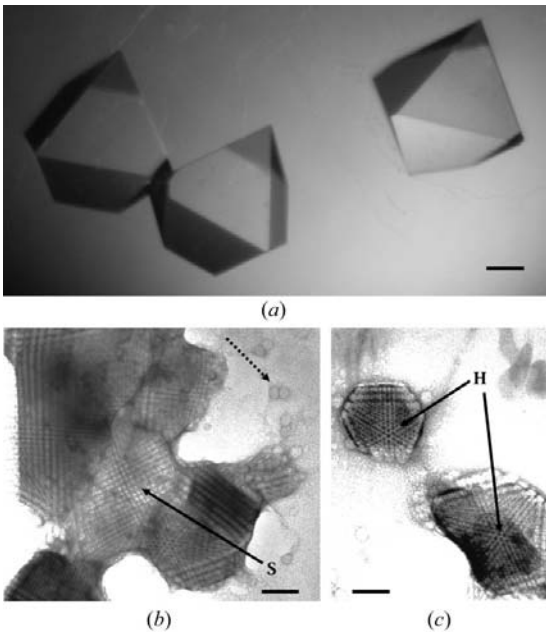

Figure 2
(*a*) Crystals of HCRSV grown in 2.9% PEG 8000, 2% 2,3-butanediol and 0.1 *M* MES pH 6 at 288 K. The bar represents 200 µm. (*b*), (*c*) Electron micrographs of crushed HCRSV crystal fragments negatively stained with 1% uranyl acetate. The square and hexagonal patterns in the crystal fragments are indicated by 'S' and 'H', respectively. The dotted arrow indicates the release of virus particles from the crystal fragment. The bar represents 140 nm.

crystal to grow larger in size. The best crystals were produced using 2.8–3.3% PEG 8000 supplemented with 2–8% 2,3-butanediol in 0.1 *M* MES pH 6. These bipyramidal crystals grew to 0.4–0.5 mm within one week and remained stable for longer than a month (Fig. 2*a*).

A range of HCRSV concentrations between 15 and 90 mg ml^{-1} were used and the concentration was found to influence the appearance of crystals and the rate of crystal growth. By using virus concentrations of 60 and 90 mg ml^{-1}, large faceted crystals were produced. In contrast, dendrite-like crystals were observed when virus concentrations below 45 mg ml^{-1} were used. Therefore, all subsequent crystallization trials were set up using 60 mg ml^{-1} virus.

Different cryoprotectants were tested for protection of crystals under cryogenic conditions, which included glycerol, MPD and 2,3-butanediol. Direct transfer of crystals into 20% cryoprotectant resulted in cracking of the crystals. As an alternative approach, crystals were soaked in increasing concentrations of the cryoprotectant solution in 5% increments from 5 to 30% for 3 min at each step. The crystals were then frozen immediately in liquid nitrogen for storage or frozen directly in a 100 K N_2-gas stream prior to X-ray data collection. The best cryoprotectant was 2,3-butanediol, with which the crystals diffracted to at least 4.5 Å with synchrotron radiation. Non-frozen crystals did not diffract to higher resolution, suggesting that the relatively low resolution obtained was not a consequence of the freezing conditions, but rather of intrinsic disorder in the crystals.

Observation of crushed crystals under the EM revealed virus particles that were arranged in a regular array (Fig. 2*b*). Square (Fig. 2*b*) and hexagonal (Fig. 2*c*) patterns were observed, indicative of closely packed virus particles and consistent with a cubic space group.

The best crystals diffracted to at least 4.5 Å resolution (Fig. 3*a*). The crystal data could be processed in the cubic space group *P*23, with unit-cell parameter a = 392 Å and $R_{\rm merge}$ = 16.5% including all data to 4.5 Å resolution. However, beyond about 5 Å the data quality was poor (Table 1). From packing considerations, there should be two particles in the unit cell, located at positions $(x, y, z) = (0, 0, 0)$ and $(\frac{1}{2}, \frac{1}{2}, \frac{1}{2})$ and rotated by 90° relative to one another. This arrangement was confirmed by self-rotation functions with $\kappa = 72°$, which showed two sets of peaks corresponding to icosahedral symmetry, one rotated by 90° relative to the other (Fig. 3*b*).

At present, work is under way to improve the crystal quality and increase the resolution of the diffraction data. Preliminary indications suggest that sample heterogeneity may be the cause of the crystal disorder. Once good data are available, the HCRSV structure will be determined using the structure of TBSV as a starting model for phasing.

We thank R. Kumaresan for assistance with electron microscopy work. We are grateful to Danny Doan and Tommy Wang for help with crystal data collection and processing. This research is funded by the Agency for Science, Technology and Research (A*STAR) to TD and the NUS through research grant R-154-000-111-112 to S-MW.

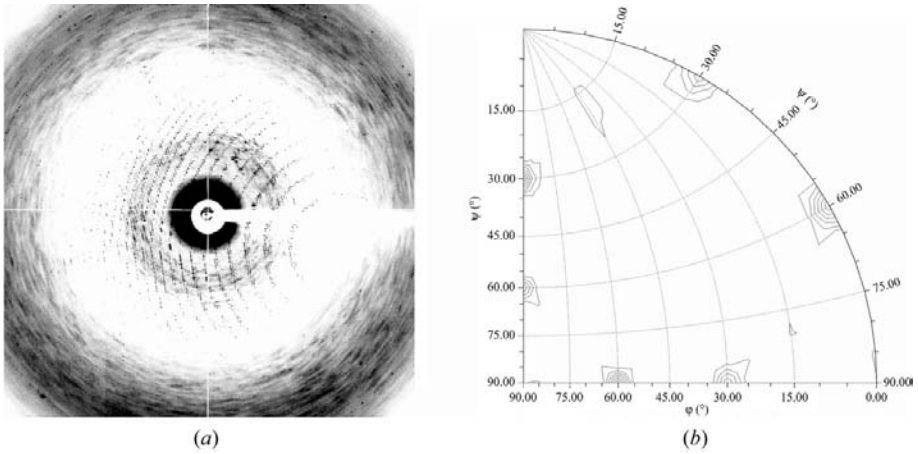

Figure 3
(*a*) Oscillation diffraction pattern from a well formed HCRSV crystal. Reflections can be observed to the edge of the image plate at 4 Å resolution, although there is a large amount of diffuse background scattering, suggesting some disorder of the crystal. (*b*) Self-rotation function for $\kappa = 72.0°$ of HCRSV data in space group *P*23 calculated between 5 and 6 Å resolution. Two sets of fivefold peaks corresponding to icosahedral symmetry can be observed. Both particles are aligned with the 222 axes of the *P*23 unit cell; each is rotated by 90° relative to the other.

References

Caspar, D. L. D. & Klug, A. (1962). *Cold Spring Harbor Symp. Quant. Biol.* **27**, 1–24.
Hogle, J. M., Maeda, A. & Harrison, S. C. (1986). *J. Mol. Biol.* **191**, 625–638.
Huang, M., Koh, D. C. Y., Weng, L., Chang, M. L., Yap, Y. K., Zhang, L. & Wong, S. M. (2000). *J. Virol.* **74**, 3149–3155.
Hurtt, S. S. (1987). *Phytopathology*, **77**, 845–850.
Johnson, J. (2001). *Alternative Agriculture: What Is Kenaf? Rural Enterprise and Alternative Development Initiative Report 1*. Carbondale, IL, USA: Southern Illinois University Carbondale.
Morris, T. J. & Carrington, J. C. (1988). *The Plant Viruses*, Vol. 3, edited by R. Koenig, pp. 73–112. New York: Plenum.
Olson, A. J., Bricogne, G. & Harrison, S. C. (1983). *J. Mol. Biol.* **171**, 61–93.
Otwinowski, Z. & Minor, W. (1997). *Methods Enzymol.* **276**, 307–326.
Tong, L. & Rossmann, M. G. (1997). *Methods Enzymol.* **276**, 594–611.
Waterworth, H. E., Lawson, R. H. & Monroe, R. L. (1976). *Phytopathology*, **64**, 570–575.
Wong, S. M. & Chng, C. G. (1992). *Phytopathology*, **82**, 722.